Elastic stiffness of $L1_0$ FePt thin film studied by picosecond ultrasonics

N. Nakamura,[1,a)] A. Uranishi,[1] M. Wakita,[1] H. Ogi,[1] M. Hirao,[1] and M. Nishiyama[2]
[1]*Graduate School of Engineering Science, Osaka University, Toyonaka, Osaka 560-8531, Japan*
[2]*Renovation Center of Instruments for Science Education and Technology, Osaka University, Toyonaka, Osaka 560-0043, Japan*

(Received 29 September 2010; accepted 10 February 2011; published online 11 March 2011)

The elastic stiffness of epitaxial and polycrystalline $L1_0$ FePt films is studied by picosecond ultrasonics coupled with x-ray reflectivity analysis, and we find that C_{33} of $L1_0$ FePt is 309 GPa. The morphology of FePt films shows dependence on the film thickness; as the film thickness increases the mazelike structure changes to a continuous film. The elastic stiffness correlates with the morphology change, and it increases as the film thickness increases. When the film thickness exceeds 40 nm, the elastic stiffness becomes independent of the film thickness, and we define the saturated value as C_{33} of $L1_0$ FePt. © *2011 American Institute of Physics*. [doi:10.1063/1.3562031]

$L1_0$ FePt shows a chemically ordered face-centered tetragonal structure, which consists of stacks of alternating monatomic layers of Fe and Pt in the [001] direction. It shows high uniaxial magnetic anisotropy in the [001] direction, $K_u = 7.0 \times 10^6$ J/m^3 at room temperature,[1] making it a candidate for high-density magnetic recording media. Considerable attention has been focused on $L1_0$ FePt, and the relationship between crystallographic structure, morphology, and magnetic properties have been investigated intensively while varying the fabrication conditions. Despite numerous studies on $L1_0$ FePt, the elastic properties remain unknown. Although the elastic constant is a fundamental parameter to be determined when a material is found or developed, that of $L1_0$ FePt has not yet been measured experimentally. A possible reason for this is the difficulty of fabricating a sufficiently large single crystal of $L1_0$ FePt that the elastic constants can be accurately determined by conventional methods. In the literature, elastic constants of $L1_0$ FePt have been deduced using the modified embedded-atom method (MEAM),[2] *ab initio* calculations,[3,4] and the analytic bond-order potential (ABOP) formalism.[3] However, the calculated values vary widely depending on the calculation method and the calculation conditions; for example, the component C_{33} of the elastic constant matrix ranges from 242 to 371 GPa.[2–4] Because elastic constants are defined as the second-order derivative of the interatomic potential, this variation implies that a reliable potential has not yet been identified. As a result, other physical properties calculated by these methods could be unreliable. Comparison between calculated and measured elastic constants is a possible way to define a reliable potential, and measuring the elastic constant is indispensable for this task.

In this letter, the elastic constants of epitaxial $L1_0$ FePt film is determined using picosecond ultrasonics coupled with x-ray reflectivity analysis.[5] This technique is capable of determining the elastic constant of a film thinner than 100 nm using a femtosecond-pulsed laser, and has been applied for several thin films.[6–9] In epitaxial growth of $L1_0$ FePt films, a remarkable change in the morphology occurs; with increasing film thickness, isolated particles grow, and coalesce, forming a continuous film.[10] Because macroscopic elastic constants of thin films tend to be different from those of the corresponding bulk materials due to nanoscale defects,[11–14] the contribution of these defects to the elastic constants must be considered carefully. In this study, we investigate the relationship between the elastic constants and morphology while varying the total film thickness, and determine the elastic constant of single crystal $L1_0$ FePt. Finally, we compare the experimentally determined elastic constants with reported calculated values.

$L1_0$ FePt films were prepared by depositing a Fe/Pt superlattice on heated substrates referring to the literature.[15,16] Superlattices were deposited on MgO(001) and borosilicate glass substrates heated to 500 °C. After depositing a 3.6-Å-thick Pt buffer layer, Fe and Pt were deposited alternately. The thickness of each layer was 2.8 Å and 3.6 Å, respectively. The total film thickness was varied between 17 and 73 nm by changing the number of bilayers. The crystal structure was investigated by x-ray diffraction measurements, and the film thickness, d, was determined by x-ray reflectivity analyses.[17,18] The morphology was investigated by the atomic-force microscopy (AFM). For evaluating the effect of the fabrication method on the elastic constants, we also prepared an $L1_0$ FePt film by cosputtering. This film was prepared by depositing Fe and Pt simultaneously via rf-magnetron sputtering onto a MgO(001) substrate at 700 °C. The film thickness was 107 nm. The composition of these films was identified to be $Fe_xPt_{100-x}(x = 50 \pm 10)$ by atomic absorption spectrometry.

The elastic constants of FePt thin films were determined using picosecond ultrasonics. Picosecond ultrasonics is a technique to generate and detect a gigahertz-frequency longitudinal acoustic pulse propagating in the film-thickness direction using ultrashort pulses of light.[19,20] This technique is capable of measuring the round-trip time, Δt, of the acoustic phonon during repeated reflections between the film surface and the film-substrate interface. The out-of-plane longitudinal elastic constant, $C_\perp$, is determined from Δt, d, and the mass density, ρ, by the relation $C_\perp = \rho(2d/\Delta t)^2$. ρ was calculated from the atomic weights and lattice parameters of $L1_0$ FePt. In very thin films, a fundamental standing phonon oscillation was detected instead of multiple reflections of acoustic phonons. In this case, $C_\perp$ is determined from the resonance frequency, f, by $C_\perp = \rho(2df)^2$. We used a 15 mW

a)Electronic mail: nobutomo@me.es.osaka-u.ac.jp.

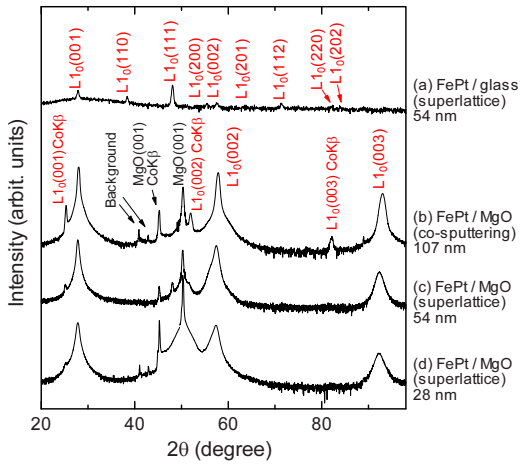

FIG. 1. (Color online) X-ray diffraction spectra of (a) the polycrystalline FePt film, (b) the epitaxial film prepared by the co-sputtering, and epitaxial films prepared by depositing superlattice with (c) 54 nm and (d) 28 nm.

800-nm-wavelength pulsed laser for generation and a 5 mW 400-nm-wavelength pulsed laser for detection. Details of our measurement method appear elsewhere.[5]

From the x-ray diffraction spectra in Fig. 1, it was confirmed that polycrystalline $L1_0$ FePt films were grown on glass substrates. Furthermore, the grains were randomly oriented in the film-thickness direction. On MgO(001) substrates, (001) epitaxial $L1_0$ FePt films were grown. In-plane x-ray diffraction analyses confirmed the cube-on-cube epitaxial relationship with the substrate; the (100) direction of the $L1_0$ FePt was parallel to the (100) direction of the MgO substrate (see Ref. 21).

Figure 2 shows a typical reflectivity change as measured by picosecond ultrasonics, plotted as change in reflectivity versus the time delay of the probe light. An intense peak appeared at 10 ps, indicating that an acoustic phonon was generated at this time. Following the initial peak, a train of echo signals was observed ($m=1,2,\ldots,5$), which originates from multiple reflections of the acoustic phonon in the FePt film. Δt was determined from the slope of the relationship between the time delay and m (shown in the inset in Fig. 2).

Figure 3(a) shows measured $C_\perp$ values of $L1_0$ FePt thin films. In polycrystalline films, $C_\perp$ increased asymptotically as the film thickness increased, changing by as much as 15% between the thinnest and thickest films measured. These films show random orientation of grains, and the measured $C_\perp$ corresponds to C_{11} of an isotropic aggregate, which is denoted by $\bar{C}_{11}$. AFM images confirmed that these films consist of particle grains and as the film thickness increases, the grain size increases (see Ref. 21). In polycrystalline films, weak bonds between grains soften the films. Increasing the grain size restores the elastic constants to those of the flawless bulk material.[22] Therefore, film-thickness dependence of $C_\perp$ in polycrystalline $L1_0$ FePt is attributed to the change in the volume fraction of grain boundary regions. Grain boundary regions are expected to decrease as the film thickness increases due to the coalescence of grains. When the film thickness is sufficiently large, $C_\perp$ should be consistent with the value of bulk material. In our experiments, $C_\perp$ became constant for $d>40$ nm. In Fig. 3(a), the thickness dependence of $C_\perp$ is approximated by an exponential function. By this extrapolation, $\bar{C}_{11}$ of bulk $L1_0$ FePt is expected to be 333 GPa.

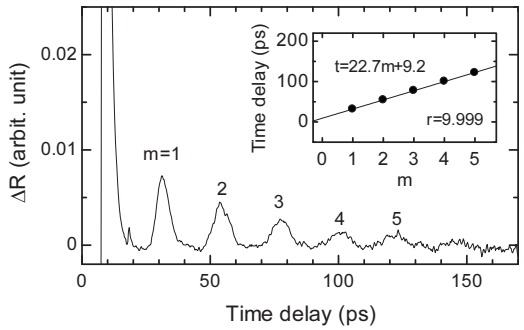

FIG. 2. Time-resolved reflectivity change in probe light in a 54-nm-thick polycrystalline $L1_0$ FePt film: multiple reflection echoes were observed ($m=1,2,\ldots,5$). Roundtrip time was determined from the slope of the time delay vs m (inset).

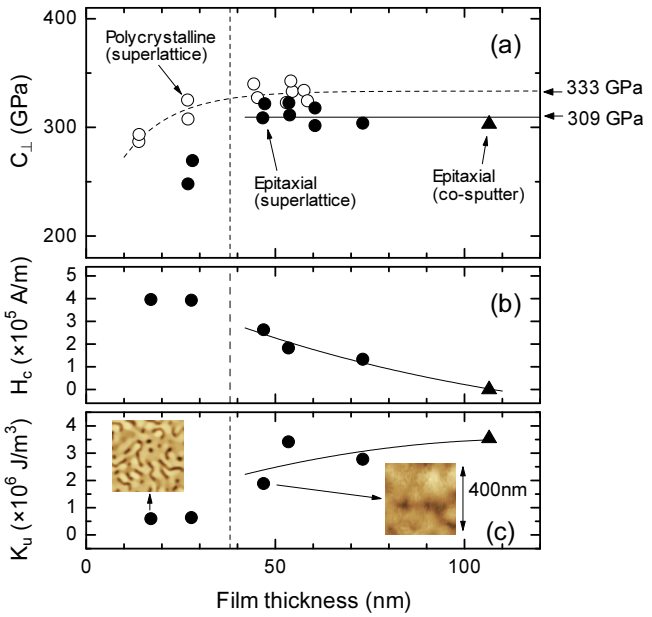

FIG. 3. (Color online) Film-thickness dependence of (a) the out-of-plane elastic stiffness $C_\perp$, (b) coercivity H_c, and (c) uniaxial magnetic anisotropy energy K_u. Open circles denote polycrystalline films deposited on glass substrates. Dots designate epitaxial films fabricated by depositing superlattices on MgO. Triangle denotes an epitaxial film prepared by co-sputtering on MgO. In (c), insets show typical AFM images.

In epitaxial films, $C_\perp$ at $d=28$ nm was significantly smaller than those of the other films, and for $d>40$ nm, $C_\perp$ was independent of the thickness. We gain insight on this behavior by comparing elastic stiffness with the AFM images and magnetic properties. For $d<30$ nm, a mazelike structure was observed [shown in the insets in Fig. 3(c)]. This structure is fabricated by coalescence of isolated particles, and the resulting films are highly defective.[10] For $d>40$ nm, the mazelike structure disappeared and continuous films were grown on MgO(001). These results indicate that there is a threshold in the film structure between 30 and 40 nm.

A threshold thickness was also observed in the coercivity H_c and the uniaxial magnetic anisotropy energy K_u as measured with a superconducting quantum interference device. For $d<30$ nm, H_c and K_u were independent of the film thickness but for $d>40$ nm they varied with the film thickness [Figs. 3(b) and 3(c)]. Shima *et al.*[10] reported that a morphology change from isolated particles to a mazelike structure significantly affects the magnetic properties and electric resistance. As the particles grow and coalesce, the

TABLE I. Comparison of determined elastic constant (GPa) to calculated values.

C_{11}	C_{12}	C_{13}	C_{33}	C_{44}	C_{66}	$\bar{C}_{11}$	$\bar{C}_{44}$	Method	Reference
			309 ± 12			333 ± 10		Picosecond ultrasonics	Present study
304	223	197	242	107	41	307	59	MEAM	Kim *et al.*[a]
261	169	151	299	103	133	310	85	*Ab initio* calculation (PAW GGA)	Müller *et al.*[b]
360	229	185	371	143	192	414	120	*Ab initio* calculation (PAW LDA)	Müller *et al.*[b]
258	203	185	293	141	182	334	87	ABOP	Müller *et al.*[b]
422	94	160	324	140	64	371	112	*Ab initio* calculation (PAW GGA)	Zotov and Ludwig[c]

[a]Reference 2.
[b]Reference 3.
[c]Reference 4.

mechanism changes from rotation of the magnetization to domain wall displacement. This causes a drastic drop in H_c. Similarly, we consider that the structure change from a mazelike structure to a continuous film caused the change in magnetic properties at the threshold thickness. Thus, magnetic properties also confirm that for $d > 40$ nm the films are very nearly flawless continuous films.

For $d > 40$ nm, a long-range order parameter S was calculated from the x-ray diffraction spectra to confirm the chemical ordering of the films. S reaches unity for perfectly ordered films, and is zero for a chemically disordered film, which is estimated from the integrated area of the fundamental (002) peak, those of the superstructure (001) and (003) peaks, and other parameters.[23] S of the films was 0.87 ± 0.13, and significant dependence on the film thickness was not observed, indicating that observed fluctuation in S does not affect $C_\perp$ seriously. In Fig. 1, diffraction peaks of the cosputtered film appear at slightly higher angles than those of the multilayered films. The difference corresponds to 0.64% difference in the interplanar distance in FePt⟨001⟩ direction. Considering the higher-order elasticity, change in the interatomic distance should affect the elastic stiffness. However, the change in $C_\perp$ is estimated to be less than 6%,[24] which is smaller than the measurement error in the resultant stiffness. For these reasons, $C_\perp$ showed dependence neither on the film thickness nor the deposition methods for $d > 40$ nm, and we determine an average value of 309 GPa, which can be considered the intrinsic C_{33} of $L1_0$ FePt.

Experimentally determined elastic constants are compared to calculated values in Table I. For purpose of comparison, $\bar{C}_{11}$ was calculated from the reported elastic constants using Hill's approximation.[25] In these reported constants, fluctuation of the values exceeded more than 10%. It should be noted that Müller *et al.*[3] and Zotov and Ludwig[4] deduced elastic constants using the same method [*ab initio* calculation using the projector-augmented wave (PAW) with the generalized gradient approximation (GGA)] but their values differ with one another. The discrepancy likely originates from differences in the calculation conditions (such as the choice of k-points). These results indicate the difficulty in calculating elastic constants. Among the reported elastic constants, those calculated by *ab initio* calculation using PAW with GGA and by ABOP are somewhat close to our measured values, which indicates that these methods are suitable for theoretically deducing the mechanical properties of $L1_0$ FePt.

We studied the relationship between the elastic stiffness, morphology, and magnetic properties of $L1_0$ FePt films, and found C_{33} of $L1_0$ FePt to be 309 GPa using picosecond ultrasonics. The crystallographic orientation of epitaxial films usually depends on that of the substrate on which they are grown. By measuring the out-of-plane elastic stiffness of these films, the other components of the elastic constant matrix could be determined. This study leads to a method for determining the elastic constants of materials of which large bulk samples cannot be fabricated.

The authors would like to acknowledge Dr. T. Takeuchi and Low Temperature Center, Osaka University, for the support of measurements of magnetic properties. We also acknowledge K. Jensen for valuable comments.

[1]O. A. Ivanov, L. V. Solina, V. A. Demshina, and L. M. Magat, Phys. Met. Metallogr. **35**, 81 (1973).
[2]J. Kim, Y. Koo, and B. J. Lee, J. Mater. Res. **21**, 199 (2006).
[3]M. Müller, P. Erhart, and K. Albe, Phys. Rev. B **76**, 155412 (2007).
[4]N. Zotov and A. Ludwig, Intermetallics **16**, 113 (2008).
[5]H. Ogi, M. Fujii, N. Nakamura, T. Yasui, and M. Hirao, Phys. Rev. Lett. **98**, 195503 (2007).
[6]H. Ogi, M. Fujii, N. Nakamura, T. Shagawa, and M. Hirao, Appl. Phys. Lett. **90**, 191906 (2007).
[7]N. Nakamura, H. Ogi, T. Yasui, M. Fujii, and M. Hirao, Phys. Rev. Lett. **99**, 035502 (2007).
[8]N. Nakamura, H. Ogi, T. Shagawa, and M. Hirao, Appl. Phys. Lett. **92**, 141901 (2008).
[9]H. Tanei, K. Kusakabe, H. Ogi, N. Nakamura, and M. Hirao, Appl. Phys. Lett. **95**, 011902 (2009).
[10]T. Shima, K. Takanashi, Y. K. Takahashi, and K. Hono, Appl. Phys. Lett. **81**, 1050 (2002).
[11]N. Nakamura, H. Ogi, and M. Hirao, Acta Mater. **52**, 765 (2004).
[12]H. Ogi, N. Nakamura, H. Tanei, M. Hirao, R. Ikeda, and M. Takemoto, Appl. Phys. Lett. **86**, 231904 (2005).
[13]H. Ogi, T. Shagawa, N. Nakamura, M. Hirao, H. Odaka, and N. Kihara, Phys. Rev. B **78**, 134204 (2008).
[14]N. Nakamura, Y. Kake, H. Ogi, and M. Hirao, J. Appl. Phys. **108**, 043525 (2010).
[15]Y. Endo, N. Kikuchi, O. Kitakami, and Y. Shimada, J. Appl. Phys. **89**, 7065 (2001).
[16]F. Casoli, F. Albertini, L. Pareti, S. Fabbrici, L. Nasi, C. Bocchi, and R. Ciprian, IEEE Trans. Magn. **41**, 3223 (2005).
[17]H. Kiessig, Ann. Phys. **402**, 769 (1931).
[18]L. G. Parratt, Phys. Rev. **95**, 359 (1954).
[19]C. Thomsen, J. Strait, Z. Vardeny, H. J. Maris, J. Tauc, and J. J. Hauser, Phys. Rev. Lett. **53**, 989 (1984).
[20]C. Thomsen, H. T. Grahn, H. J. Maris, and J. Tauc, Phys. Rev. B **34**, 4129 (1986).
[21]See supplementary material at http://dx.doi.org/10.1063/1.3562031 for the in-plane x-ray diffraction spectra and AFM images.
[22]H. Tanei, N. Nakamura, H. Ogi, M. Hirao, and R. Ikeda, Phys. Rev. Lett. **100**, 016804 (2008).
[23]B. E. Warren, *X-ray Diffraction* (Addison-Wesley, Massachusetts, 1990).
[24]N. Nakamura, H. Ogi, and M. Hirao, Phys. Rev. B **77**, 245416 (2008).
[25]R. Hill, J. Mech. Phys. Solids **11**, 357 (1963).